PERGAMON

Deep-Sea Research II 47 (2000) 227–257

DEEP-SEA RESEARCH
PART II

Variations in bioturbation across the oxygen minimum zone in the northwest Arabian Sea

Craig R. Smith[a,*], Lisa A. Levin[b], Daniel J. Hoover[a], Gary McMurtry[a], John D. Gage[c]

[a]*Department of Oceanography, University of Hawaii, 1000 Pope Road, Honolulu, HI 96822, USA*
[b]*Marine Life Research Group, Scripps Institution of Oceanography, La Jolla, CA, 92093-0218, USA*
[c]*Scottish Association for Marine Science, Dunstaffnage Marine Laboratory, PO Box 3, Oban, Argyll, PA34 4AD, UK*

Received 28 January 1999; received in revised form 25 March 1999; accepted 30 March 1999

Abstract

Oxygen minimum zones are expected to alter substantially the nature, rates and depths of bioturbation along continental margins, yet these effects remain poorly studied. Using excess ^{210}Pb profiles, sediment X-radiography and box-core samples for macrofauna, we examined bioturbation processes at six stations (400, 700, 850, 1000, 1250 and 3400 m deep) along a transect across the oxygen minimum zone (OMZ) on the Oman margin. Bottom-water oxygen concentrations ranged from ~ 0.13 ml l^{-1} at 400 m to ~ 2.99 ml l^{-1} at 3400 m. ^{210}Pb mixed-layer depth and bioturbation intensity (D_b) exhibited high within-station variance, and means did not differ significantly among stations. However, the mean mixed-layer depth (4.6 cm) for pooled OMZ stations (400–1000 m depths, 0.13–0.27 ml l^{-1} bottom-water oxygen) was half that for stations from similar water depths along well-oxygenated Atlantic and Pacific slopes (11.1 cm), suggesting that oxygen stress reduced ^{210}Pb mixing depth on the Oman margin. Modal burrow diameter and the diversity of burrow types at a station were highly correlated with bottom-water oxygen concentration from the edge to the core of the Oman OMZ (Spearman's rho $\geqslant 0.89$, $p \leqslant 0.02$), suggesting that these parameters are useful proxies for bottom-water oxygen concentrations under dysaerobic conditions. In contrast, neither the maximum diameter and nor the maximum penetration depth of open burrows exhibited oxygen-related patterns along the transect. Reduced ^{210}Pb mixing depth within the Oman-margin OMZ appeared to result from a predominance of surface-deposit feeders and tube builders within this zone, rather than from simple changes in horizontal or vertical distributions of macrofaunal abundance or biomass. The number of burrow types per station was highly correlated with macrofaunal species diversity, suggesting that burrow diversity may be a good

* Corresponding author. Fax: 001-808-956-9516.
E-mail address: csmith@soest.hawaii.edu (C.R. Smith)

PII: S0967-0645(99)00108-3

proxy for species diversity in paleo-dysaerobic assemblages. We conclude that bottom-water oxygen concentrations of 0.13–0.27 ml l^{-1} substantially alter a number of bioturbation parameters of importance to diagenetic and biofacies models for continental margins.

1. Introduction

Bioturbation, or the displacement of sediment particles by animals, results from feeding, burrowing and habitat construction by benthos (e.g., Wheatcroft et al., 1990). These bioturbation activities have many direct and indirect effects on seafloor sediments. Simple nonselective biogenic movement of particles within the sediment column, such as may result from burrowing, alters particle exposure to fluid shear stress, redox conditions, and microbial metabolism, thus influencing chemical reaction rates and burial efficiency (e.g., Aller, 1982; Jumars and Nowell, 1984; Wheatcroft et al., 1990). Deposit feeding frequently alters particle composition, in situ grain size and sediment erodability (e.g., Jumars and Nowell, 1984), and can yield selective rapid subduction and/or mixing of organic-rich phytodetritus (e.g., Graf, 1989; Smith et al., 1993,1996,2000; Levin et al., 1997). Thus, the intensity and depth of bioturbation can dramatically influence the rates and depths of organic-carbon degradation (e.g., Emerson, 1985; Rabouille and Gaillard, 1991; Hammond et al., 1996) and silica dissolution (Schink et al., 1975), and the proportion of sedimenting organic carbon, pollutants, and other redox-sensitive species sequestered within the seafloor (e.g., Emerson, 1985; Rabouille and Gaillard, 1991; Kramer et al., 1991; Aller, 1990). In addition, bioturbation smears the sediment record, complicating the reconstruction of pollution histories and paleoclimates from deposited tracers (e.g., Wheatcroft, 1990; Savrda and Bottjer, 1991; Kramer et al., 1991).

These bioturbation processes are expected to change substantially with declining bottom-water oxygen as benthic communities become oxygen stressed (e.g., Pearson and Rosenberg, 1978; Rhoads et al., 1978; Diaz and Rosenberg, 1995). However, we presently have limited understanding of the influence of oxygen gradients on bioturbation along continental margins. Most information concerning oxygen-bioturbation relationships along margins comes from ichnological studies, in which the effects of bioturbation on sedimentary fabric have been used to reconstruct paleo-oxygenation histories of marine systems. In particular, characteristic assemblages of trace fossils, body fossils and sediment laminations, called "biofacies", have been used to infer relative levels and rates of change of bottom-water oxygenation (e.g., Savrda and Bottjer, 1991). These biofacies models predict a decrease in the size, abundance, diversity and penetration depth of infaunal traces, as well as an increasing occurrence of primary laminations, as bottom-water oxygen decreases below a threshold level (e.g., Savrda and Bottjer, 1991). A shift in infaunal lifestyles between subsurface-feeding and surficial-sediment-grazing assemblages (i.e., between formers of fodinichnia and pascichnia) also has been predicted, although the direction of this change as oxygen decreases is controversial (Ekdale and Mason, 1988,1989; Wheatcroft, 1989). Recent recognition that oxygen stress may yield subtle gradations in community

structure has led to the delineation of five oxygen-related biofacies characterized by decreasing intensities and depths of bioturbation: aerobic, dysaerobic, exaerobic, quasi-anaerobic and anaerobic (Savrda and Bottjer, 1991). The bottom-water oxygen concentrations thought to bound these biofacies are only roughly characterized (see Table 7 in Levin et al., 2000), with the initiation of oxygen effects on bioturbation (i.e., the aerobic/dysaerobic boundary) thought to occur between 0.3 and 1.0 ml l^{-1}. This biofacies model is based largely on studies along the California, USA, margin and requires validation in other oceanographic settings. The sharp gradients in bottom-water oxygen concentration observed at the boundaries of oxygen-minimum zones (OMZs) on some continental margins, such as in the Arabian Sea, provide excellent opportunities to evaluate the relationships between oxygen concentrations and bioturbation processes, and to test biofacies models.

Steep oxygen gradients occurring at the upper and lower boundaries of OMZs often appear to support enhanced biological activity, both in the water column (e.g., Karl and Knauer, 1984; Lipschultz et al., 1990; Wishner et al., 1990,1995) and in the benthos (Mullins et al., 1985; Thompson et al., 1985; Levin et al., 1991). Possible explanations include (1) elevated microbial metabolism and production, both aerobic and anaerobic, due to oxidation of accumulated reduced compounds, and (2) elevated densities of animals able to exploit aerobically high food availability just above their O_2-tolerance threshold (Levin et al., 1991). A dramatic shift from minimal to extensive bioturbation might thus be expected across OMZ boundaries. The relationships between oxygen concentration and animal body size, density, feeding habits and depth distributions appear likely to determine the extent of this change.

In this paper, we examine patterns of bioturbation along a transect across the OMZ boundary on the Oman margin in the Arabian Sea (Fig. 1). In our study area, bottom-water oxygen concentrations drop abruptly from 3 to ~ 0.1 ml l^{-1} at a water depth of ~ 100 m, rise gradually to 1 ml l^{-1} at ~ 1500 m, and once again reach ~ 3 ml l^{-1} below water depths of 3000 m (Fig. 2). Based on biofacies models and studies of faunal changes across OMZs (Levin et al., 1991,2000; Wishner et al., 1990,1995), we consider the OMZ boundary to fall at oxygen levels between 0.3 and 1.0 ml l^{-1}. Our transect ranges from ~ 400 to ~ 3400 m depth, i.e. from the core of the OMZ, across its lower boundary and into well-oxygenated abyssal waters.

Here we use excess ^{210}Pb profiles, sediment X-radiography, and box-core samples of macrofauna to test the following hypotheses derived from biofacies models and previous OMZ studies.

(1) The intensity of mixing, as measured by the eddy diffusion coefficient D_b, and the mixed layer depth for excess ^{210}Pb are maximal at the OMZ boundary and decline into the OMZ.
(2) The diameter (maximum and modal), diversity and penetration depth of open animal burrows are positively correlated with bottom-water oxygen concentration from the boundary to the core of the OMZ.
(3) The above changes in bioturbation are correlated with a shoaling in the depth distribution of macrofauna, decreases in macrofaunal community abundance and biomass, and a shift to surface-oriented life-styles near the OMZ core.

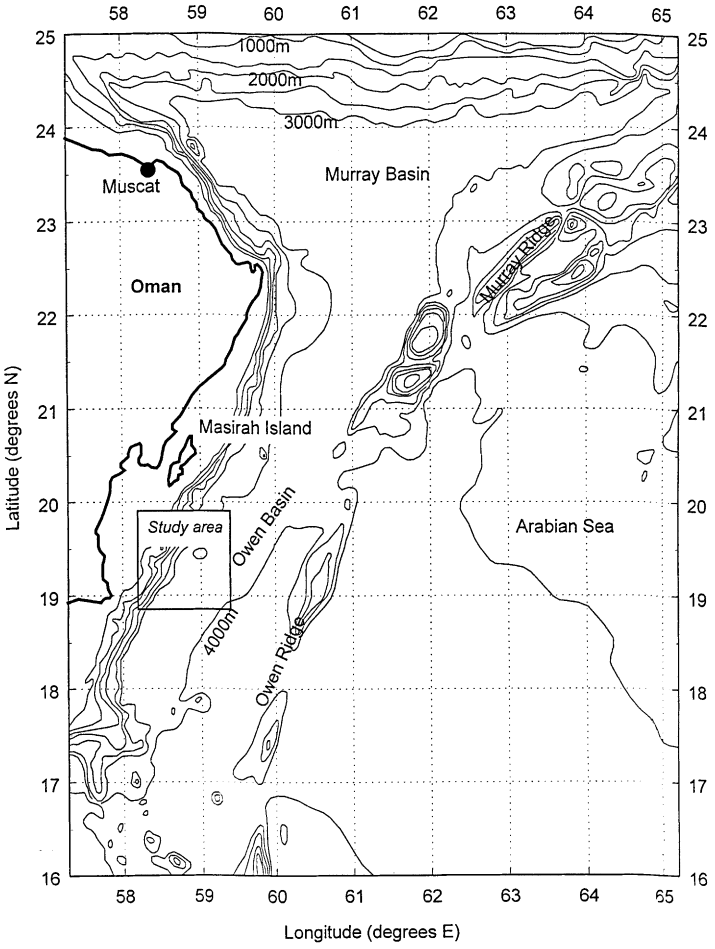

Fig. 1. Area studied for this paper during *Discovery* Cruise 211 on the Oman Margin.

We find that certain parameters, e.g., modal burrow size and diversity, show significant changes across the OMZ while other parameters, in particular mixing intensity of ^{210}Pb, exhibit little correlation to changes in bottom-water oxygen concentrations.

2. Study site and methods

2.1. Study site

Data were collected along the Oman Margin in the northwest Arabian Sea (roughly 19°21′ N, 48°15′E) during October and November 1994 on the RRS *Discovery* Cruise

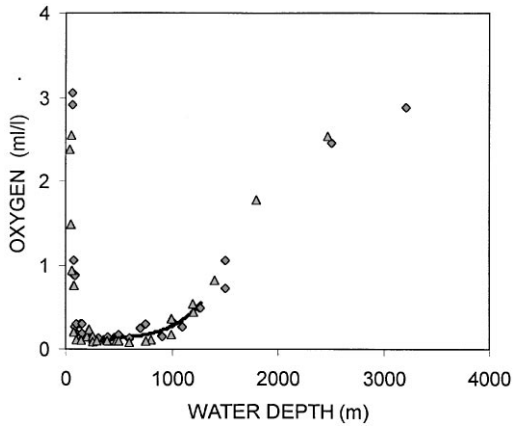

Fig. 2. Composite profile of oxygen from *Discovery* Cruises 210 and 212 used for this study (see text for explanation). The curve shown is a second-order polynomial fitted to the data between 250 and 1500 m depths, and used to provide the best estimate for oxygen values at our 400–1250-m stations. The equation for the curve is: oxygen concentration $= 0.05919(\text{depth})^{0.1312} + (4.864 \times 10^{-16})(\text{depth})^{4.804}$, with $r^2 = 0.9104$. Points marked by triangles are from *Discovery* 210 (Sept. 94) and diamonds are from *Discovery* 212 (Nov. 94).

211. A total of six stations were studied at waters depths of approximately 400, 700, 850, 1000, 1250 and 3400 m (Table 1). The physical characteristics of these stations are presented in Table 2. Based on our best and minimum estimates of bottom-water oxygen concentrations, our 400–700 m stations fall within the OMZ, the 1250-m station is at its boundary, and the 3400-m station is well below the OMZ.

Bottom-water oxygen data for our stations were obtained as follows. Measurements made during *Discovery* Cruise 211 from multiple-core topwater and Niskin bottles appeared to be faulty (variance was inordinately high), possibly due to sampler leakage or heat-spoiled reagents. We thus used bottom-water oxygen data collected from hydrocasts during *Discovery* Cruises 210 and 212 (in September and November, respectively) to the Oman margin (Burkill, 1998). Winkler titration data from three stations within 9 km of our margin transect (stations AS 1 at 19°15.0′N, 58°35.4′E, AS 2 at 19°16.5′N, 58°32.2′E and AS 3 at 19°13.3′N, 58°20.6′E) were used to estimate oxygen values at our stations from 400 and 1250 m depths. One cast from each of these stations was obtained in both Sept. and Nov. 1994, yielding the data from 250 to 1800 m in Fig. 2. We fitted a second-order polynomial to these data between 250 and 1500 m to obtain the best estimate of bottom-water oxygen concentrations at our station depths of 400, 700, 850, 1000 and 1250 m (Table 1). For depths below 1800 m, oxygen concentrations were taken directly from measurements made during four hydrocasts at station A1 (depth = 3397 m, 19°00.0′N, 59°00.0′E), which is a few kilometers from our abyssal station; two casts were made at station A1 in Sept. and two in Nov. 1994. We believe it is appropriate to use oxygen data integrating month-long time scales because we expect macrofauna and bioturbation processes to respond either to mean or minimum bottom-water oxygen concentrations over time scales of weeks to months.

Table 1
Samples collected for this study. All samples were collected between 9 October and 11 November. MC = multiple core, Veg = vegematic subcore, BC = box core, XR = x-ray, MF = macrofauna, PB = ^{210}Pb profile.

Nominal station depth (m)	Sample no.	Sample water depth (m)	Latitude °N	Logitude °E	Data type
400	12690/1	377			MC, PB
	12692/4	398	19°22′	58°15′	BC, XR
	12698/1	401	19°21.78′	58°15.49′	BC, MF
	12695/4	406	19°21.92′	58°15.49′	BC, MF
	12695	412	19°22′	58°15′	MC, PB
	12695/7	414	19°21.83′	58°15.42′	BC, MF, XR
	12690/3	418	19°22.00′	58°15.46′	BC, MF, XR
700	12685	667	19°18′	58°17′	MC, PB
	12685/1	674	19°18.95′	58°15.53′	BC, MF
	12682/2	685	19°19′	58°16′	MC, PB
	12685/8	690	19°18.66′	58°15.64′	BC, MF, XR
	12685/6	700	19°18.88′	58°15.46′	BC, MF, XR
	12682/3–2	742	19°18′	58°17′	MC, PB
	12683/3–7	742	19°18′	58°17′	MC, PB
	12685/10	746	19°18.72′	58°15.79′	BC, XR
850	12713	823	19°14′	58°23′	MC, PB
	12711	833	19°14′	58°23′	MC, PB
	12711/2	840	19°14.21′	58°23.11′	BC, MF, XR
	12713/1	850	19°14.35′	58°23.16′	BC, MF, XR
	12713/5	854	19°14.14′	58°23.01′	BC, MF
	12713/4	862	19°14.16′	58°23.13′	BC, MF, XR
	12715/1	874	19°14.60′	58°22.97′	BC, MF, XR
1000	12722/4	963	19°16.28′	58°29.25′	BC, MF
	12722	972	19°16′	58°29′	MC, PB
	12718	981	19°16′	58°29′	MC, PB
	12718/4	982	19°16.87′	58°29.81′	BC, MF, XR
	12718/1	983	19°16′	58°29′	MC, PB
	12718/2	992	19°16.62′	58°29.77′	BC, MF, XR
	12722/1	992	19°16.09′	58°29.68′	BC, MF, XR
	12716/2	996	19°16.05′	58°29.08′	BC, MF, XR
1250	12725/6	1244	19°14.31′	58°29.25′	BC, MF
	12723	1252	19°14′	58°29′	MC, PB
	12725/2	1265	19°14.03′	58°29.29′	BC, MF, XR
	12723/2	1285	19°14.02′	58°29.42′	BC, MF, XR
	12723/4	1291	19°14.25′	58°29.55′	BC, MF, XR
	12725	1296	19°14′	58°29′	MC, PB
	12725/4	1310	19°13.91′	58°31.63′	BC, MF, XR
3400	12687/4	3360	18°59.84′	59°00.96′	BC, MF, XR
	12687/1	3372	18°59.51′	59°00.76′	BC, MF
	12688/1	3384	19°00′	59°01′	BC, XR
	12671/4	3392	19°00.29′	59°00.22′	BC, MF, XR

Table 1 (*continued*)

Nominal station depth (m)	Sample no.	Sample water depth (m)	Latitude °N	Logitude °E	Data type
	12671	3392	19°00′	59°01′	MC, PB
	12687/9	3392	18°59.77′	59°00.49′	BC, MF
	12687	3393	19°00′	59°01′	MC, PB
	12730/1	3400	18°00.72′	59°59.41′	BC, MF

2.2. Methods

Excess ^{210}Pb profiles were measured from 5.7-cm diameter tube cores collected with a multiple corer similar to that described by Barnett et al. (1984). Station data are presented in Table 1. Once on shipboard, multiple-core tubes were extruded and sectioned at 1-cm intervals to a depth of 10 cm, and then at 2-cm intervals to the bottom of the core, using the methods of Pope et al. (1996). In particular, to avoid contamination from downcore smearing during the extrusion process, the outer $\sim$ 5-mm thick "rind" of each sediment interval was carefully cut away and discarded. Equivalent depth intervals from two core tubes from each lowering were then combined to yield adequate sample mass, and then double sealed in ziplock bags. In the laboratory, uranium-series activities were determined by non-destructive gamma spectrometry using an extended-range, coaxial, high-purity Ge detector (EG&G Ortec Gamma-X) with spectrum acquisition on a PC-based 4096-channel multichannel analyzer. Sediment samples were analyzed wet, sealed in counting vials, and incubated for at least 24 days to assure secular equilibrium of the short-lived daughters of ^{226}Ra. Subsequent to counting, the samples were oven-dried at 110°C for at least 48 h to obtain constant dry weights and sample porosities. Samples were corrected for counting vial geometry and for self-absorption of ^{210}Pb after methods previously described (Kim and Burnett, 1983; Kim and McMurtry, 1991). Spectral data were subsequently manipulated by computer and the reported net specific activities, normalized to NBS and EPA standards, decay-corrected to the date of sample collection. Excess ^{210}Pb activities are reported as the difference between total ^{210}Pb and ^{226}Ra activities.

In general, depth intervals were assayed for excess ^{210}Pb activity in the order 0–1, 1–2, 2–3, 4–5, 6–7, 10–12, 14–16 cm until two successive intervals yielded zero excess activity. In some cases, additional or alternative intervals were measured to elucidate irregularities in profiles. Two to four ^{210}Pb profiles were measured from each station.

To evaluate mixed-layer depths and D_b from ^{210}Pb profiles, log-linear plots of excess ^{210}Pb profiles were examined (Fig. 3). The ^{210}Pb mixed-layer depth was taken to be the depth at which a major decrease (i.e. break) in the slope of the profile was evident; in two samples (nos. 12695/2 and 12682/3–7), subsurface maxima made selection of this break point problematic. We used a similar approach to evaluate mixed-layer depths for published excess ^{210}Pb profiles from well-oxygenated slopes to

Table 2
Physical characteristics of stations sampled on the Oman margin in October–November 1994 for this study. All but the oxygen data are from Levin et al., 2000. For the 400–1250 m stations, the first bottom-water oxygen concentration given is the best estimate from the regression curve in Fig. 2; values in parentheses are ranges measured within 50 m of the nominal station depth

Water depth (m)	400	700	850	1000	1250	3400
Bottom-water temperature	13.3	10.8	9.6	8.6	6.7	1.7
Bottom-water oxygen (ml l^{-1})	0.13 (0.03-0.20)	0.16 (0.10-0.25)	0.20 (0.11-0.21)	0.27 (0.17-0.35)	0.52 (0.46-0.53)	2.99
Percent total organic carbon (0–0.5 cm)	4.99	4.03	4.01	1.93	2.67	2.72
Median grain size in μm (0–1 cm)	28.7	34.3	47.1	71.7	42.1	26.5
Percent sand (0–1 cm)	22.3	24.5	37.6	34.1	56.8	21.3

allow comparison to our Arabian Sea estimates. For the Arabian Sea cores, an eddy diffusive bioturbation coefficient was then estimated for the surface mixed layer (i.e., the profile points above and including the break point) using least-squares regression as in Smith et al. (1993). This model assumes (1) steady state, (2) constant porosity and eddy diffusivity within the mixed layer, and (3) that eddy diffusion controls the shape of the excess ^{210}Pb profile within the mixed-layer, i.e., that the bioturbation Peclet number is very small (Smith et al., 1993). For excess ^{210}Pb profiles exhibiting a well-defined mixed layer, we estimated a maximum sedimentation rate (S_{max}) from the non-zero points below the mixed layer, using least-squares regression and the constant activity model of Nittrouer et al. (1983/84). The sedimentation-rate estimates are upper limits because X-radiography and faunal samples suggested that some bioturbation was still occurring below the mixed-layer depths. Mean Peclet numbers (i.e., [mixed layer depth] × [sedimentation rate]/[D_b]) for the mixed layer were $\leqslant 0.4$ at five of our six stations; at 1000 m, a sedimentation rate could not be estimated, so we could not calculate a Peclet number.

The diameter, diversity and penetration depth of open burrows were evaluated from X-radiographs of slab cores ($2.5 \times 10 \times \sim 15$ cm) taken from 3 or 4 box cores from each station (Table 1). Rectangular plexiglas slab cores were either mounted inside the box corer during in situ sampling or inserted into the box core immediately after recovery. Within 1 h after box-core recovery, slab cores were X-rayed with a portable X-ray machine to produce a 1/1 image, and the film then developed on shipboard. In the laboratory, processed X-ray films were examined with a 4X hand lens on a light table. The diameters of the largest open burrow and the most common burrow size (i.e., modal burrow diameter), and the maximum penetration depth of an open burrow below the sediment–water interface were measured for each X-radiograph with a millimeter-scaled ruler; burrow diameters were measured to an accuracy of 0.5 mm, and burrow depths to an accuracy of ~ 0.5–2 cm depending on the irregularity of the sediment–water interface. In addition, the number of distinct types of open burrows was counted for each core, and the presence of primary laminations and any unusual features noted.

Macrofauna (> 300-μm) were sampled from each of the six stations with a 0.25-m^2 USNEL-type box corer containing vegematic subcorers (9.6×9.6 cm) (Table 1). Subcores were either sectioned vertically at intervals of 0–1, 1–2, 2–5, 5–10, and 15–20 cm, or were sampled from 0–20 cm. Three to five box cores were collected at each station, with two to four subcores examined from each box core. Estimates of total biomass and density for each station are based on both sets of subcores (66 in total), while vertical patterns were evaluated only from the first, horizontally sectioned set (41 subcores). On board ship, samples were preserved unsieved (0–2 cm intervals), after washing on 63-μm sieve (2–5 cm intervals), or after washing on a 300-μm sieve (5–15, 15–30, or 0–20 cm intervals), in an 8% buffered formalin/seawater solution. Samples were re-sieved in the laboratory, and the animals retained on a 300-μm mesh picked, identified to lowest possible taxon, and weighed wet. Our analyses do not include the traditional "meiofaunal" taxa such as nematodes, copepods, ostracods and foraminifera. For more details of macrofaunal sampling and processing, see Levin et al. (2000). Abundance, biomass and vertical distribution data for the macrofauna were

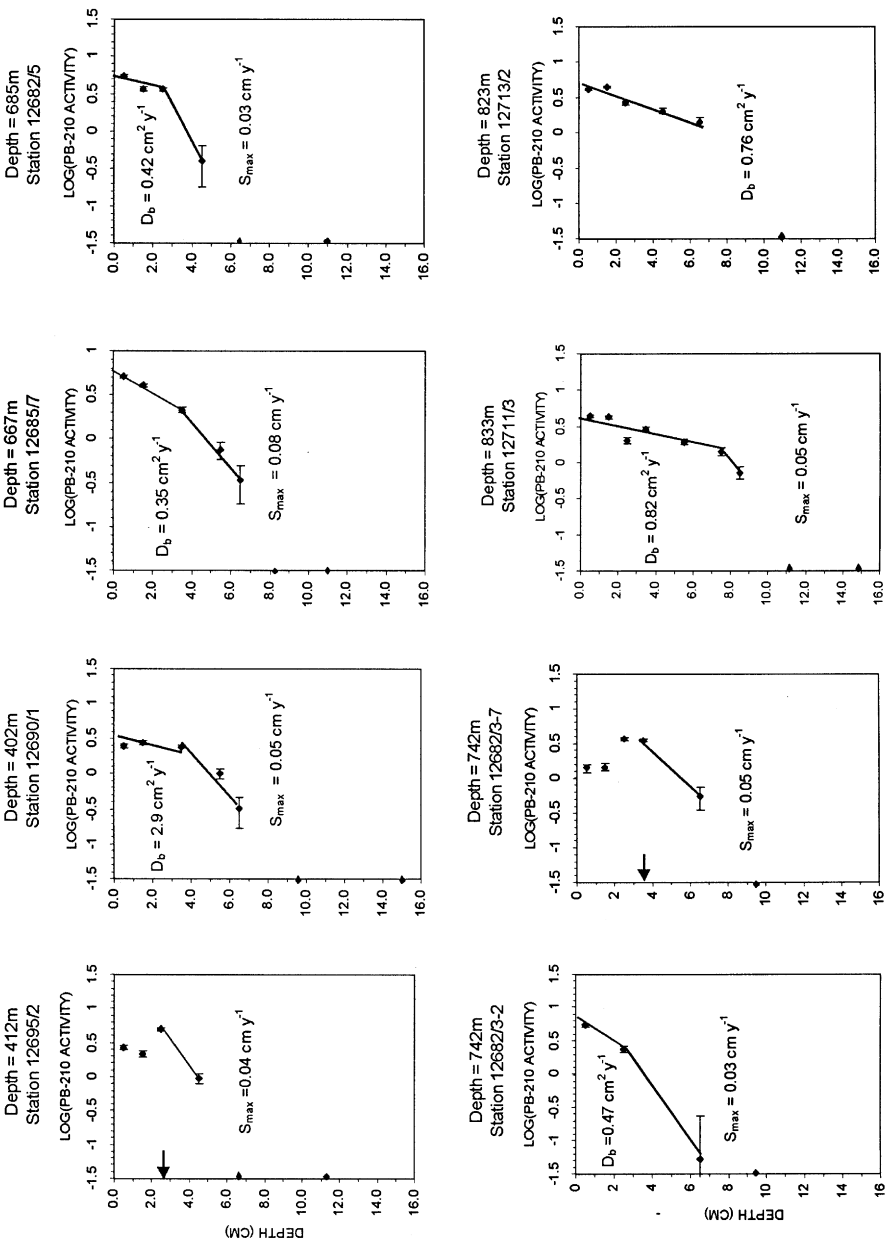
Depth = 412m
Station 12695/2
LOG(PB-210 ACTIVITY)
S_{max} =0.04 cm y^{-1}
DEPTH (CM)
Depth = 402m
Station 12690/1
D_b = 2.9 cm^2 y^{-1}
S_{max} = 0.05 cm y^{-1}
Depth = 667m
Station 12685/7
D_b = 0.35 cm^2 y^{-1}
S_{max} = 0.08 cm y^{-1}
Depth = 685m
Station 12682/5
D_b = 0.42 cm^2 y^{-1}
S_{max} = 0.03 cm y^{-1}
Depth = 742m
Station 12682/3-2
D_b =0.47 cm^2 y^{-1}
S_{max} = 0.03 cm y^{-1}
Depth = 742m
Station 12682/3-7
S_{max} = 0.05 cm y^{-1}
Depth = 833m
Station 12711/3
D_b = 0.82 cm^2 y^{-1}
S_{max} = 0.05 cm y^{-1}
Depth = 823m
Station 12713/2
D_b = 0.76 cm^2 y^{-1}

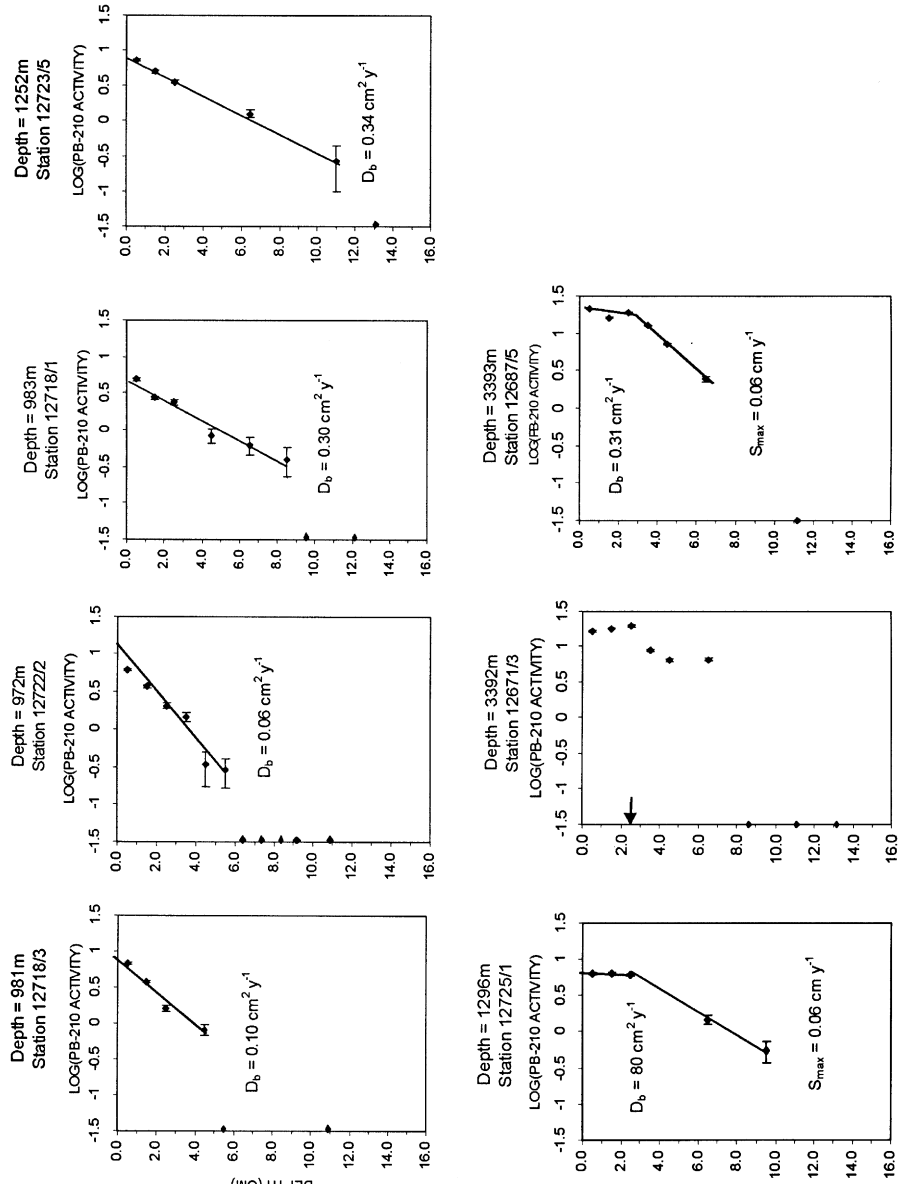

Fig. 3. Profiles of excess ^{210}Pb activity (dpm g^{-1} dry wt.) versus sediment depth for multiple-core samples. Values plotted on the vertical axes have zero activity. The regression lines were fitted to calculate the eddy diffusion coefficients (D_b). The bottom of the lines indicate the breakpoint in the profile selected as the depth of the surface mixed layer. For profiles in which a D_b was not calculated, the estimated depth of the mixed layer is indicated by an arrow. Error bars are $\pm$ one sigma from counting statistics.

calculated for each station by first averaging subcores within each box core, and then averaging box-core data within a station.

Differences among stations along the Arabian Sea transect were analyzed by ANOVA with the Tukey HSD test using JMP or Unistat software, unless a Bartlett-Box F-test indicated significant inhomogeneity of variances. For heteroscedastic data sets, differences among stations were analyzed using the Kruskal–Wallis test with Unistat software. Percentage data were arcsine transformed prior to analysis to normalize distributions. Differences between means for oxygenated slopes versus the Arabian Sea OMZ were evaluated with the t test (Dixon and Massey, 1969). Because data sets were not expected to be normally distributed, correlation analyses were conducted using the non-parametric Spearman's rho with Unistat software. Exploratory least-squares regressions were conducted using JMP software on $\log_{10}$-transformed data. An α level of 0.05 was used throughout as the criterion for statistical significance.

3. Results

3.1. Depth and intensity of ^{210}Pb mixing

Excess ^{210}Pb profiles for each station are shown in Fig. 3. Mean ^{210}Pb mixed-layer depth varied more than two-fold between stations, but these between-station differences were not statistically significant (Fig. 4, Tables 3 and 4). Lack of statistical significance could have been due to β error resulting from the small number of profiles

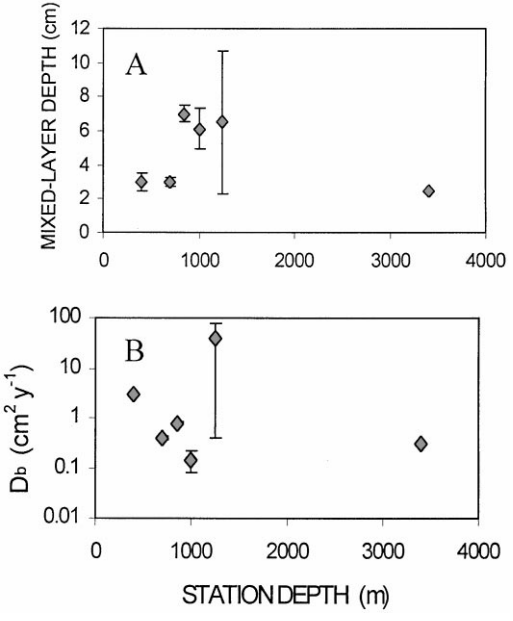

Fig. 4. (A) Mean ^{210}Pb mixed-layer depth and (B) mean ^{210}Pb bioturbation coefficient (D_b) versus depth along the Oman margin. Error bars are $\pm$ one standard error.

Table 3
Average mixed-layer depths, bioturbation coefficients within the mixed layer (D_b), and maximum sedimentation rates (S_{max}) from below the mixed layer for excess ^{210}Pb profiles along our transect

Station (m)	Mean mixed layer depth (m)	Standard error (n)	Mean D_b (cm^2 y^{-1})	Standard error (n)	Mean S_{max} (cm y^{-1})	Standard error (n)
400	3.0	0.5(2)	2.9	0(1)[a]	0.05	(2)
700	3.0	0.3(4)	0.41	0.03(3)[a]	0.04	(2)
850	7.0	0.5(2)	0.79	0.03(2)	0.05	0 (1)
1000	6.1	1.2(3)	0.15	0.07(3)	[b]	
1250	6.5	4.2(2)	40	40(2)	0.06	0 (1)
3400	2.5	0(2)	0.31	0(1)[a]	0.06	0 (1)

[a]One profile from this station exhibited subsurface peaks suggesting non-local and/or non-steady state mixing; no D_b was calculated for this profile.
[b] The mixed layer depth at this station was too deep to allow estimation of S_{max}.

Table 4
Results of analyses of among-station differences using one-way ANOVA or the Kruskal–Wallis test

Variable	Test	P level	Significant station differences
^{210}Pb Mixed layer depth	Kruskal–Wallis	0.14	—
^{210}Pb D_b	Kruskal–Wallis	0.12	—
Maximum burrow diameter	ANOVA	0.05[a]	1000 m < 1250 m
Modal burrow diameter	Kruskal–Wallis	0.02[a]	
Number of burrow types per core	ANOVA	0.0004[b]	1000 m < 1250 m, 1000 m < 3400 m, 400 m < 1250 m
Maximum burrow penetration depth	ANOVA	0.37	—
Macrofaunal abundance below 5 cm	ANOVA	0.0001[b]	850, 1000, 1250, and 3400 m < 700 and 400 m
Macrofaunal biomass below 5 cm	ANOVA	0.002[b]	All other stations < 700 m

[a]Significant at $\alpha = 0.05$.
[b]Significant at $\alpha = 0.005$.

per station (in many cases two). Even if we ignore the lack of statistical significance, the mixed-layer depth pattern was not as predicted; the highest thickness was well within the OMZ at 850 m, rather than at the boundary station at 1250 m, and there is no clear monotonic trend of decreasing mixed-layer thickness with distance into the OMZ. Nonetheless, mixed-layer thickness from the boundary to the core of the OMZ (400–1250 m) was moderately (although not significantly) correlated with oxygen concentration (Spearman rho = 0.667, $p > 0.1$), suggesting that between O_2 concentrations of 0.1 and 0.5 ml l^{-1}, bottom-water oxygen may exert some control on mixed-layer depth on the Arabian slope. Once again, the weakness of this pattern could well be due to the small number of data points ($n = 5$).

Bioturbation intensities (i.e., D_b) for ^{210}Pb within the surface mixed layer also failed to exhibit any strong patterns on the Oman slope (Table 3; Fig. 4). Mixing intensities

were not significantly different among stations (Table 4) nor were they positively correlated as predicted with bottom-water oxygen concentration from the boundary to the core of the OMZ (for the 400 to 1250-m stations, Spearman rho = 0.100, $p > 0.4$). While the highest individual D_b value was recorded from the OMZ boundary at 1250 m, high within-station variability in D_b suggests that substantially larger sample sizes would be required to elucidate any statistically significant patterns, such as enhanced D_b at 1250 m.

To explore further the effects of low oxygen on bioturbation, we compared the mean mixed-layer depth and bioturbation intensity for ^{210}Pb from within the Oman-slope OMZ to those of stations from similar depths along better oxygenated slopes in the Atlantic and Pacific Oceans (Table 5). The pooling of our OMZ stations in this comparison provided substantially more statistical power than we could obtain within the Arabian-Sea transect alone. The mean ^{210}Pb mixed-layer depth for the oxygenated slopes (mean = 11.1 cm, s.e. = 0.5 cm) was twice that of the Oman slope OMZ (mean = 4.6 cm, s.e. = 0.2 cm), and this difference was statistically significant (Table 5). In contrast, the mean mixing intensities within the mixed layer were similar for the oxygenated-slope and Oman-slope OMZ data (0.90 and 1.1, respectively, s.e. $\geqslant 0.32$ cm; Table 5). These results suggest that bottom-water oxygen levels between ~ 0.1 and ~ 0.3 ml l^{-1} on the Oman slope yield a decrease in the thickness of the mixed layer, but had no clear impact on the intensity of mixing within this layer.

3.2. X-radiographic analyses

Brief descriptions of X-radiographs from each core are presented in Table 6, and representative X-radiographs are presented in Fig. 5. Sediments from the 400-m station were characterized by fine vertical burrows in the top 2–3 cm, as well as faint centimeter-scale laminations within this zone; below ~ 3 cm, sediments were quite homogeneous. Sediments from the 700-m station contained larger, vertical tubes within the top 3–7 cm; many of these were ampeliscid amphipod tubes that protruded through the sediment–water interface. Above a sediment depth of 4–8 cm, the only visible structure was biogenic, while at depths greater than 4–8 cm, sediments often increased abruptly in density and exhibited no bioturbation; this density shift corresponded roughly to the mixed-layer depth for ^{210}Pb profiles from this station (Fig. 3). At the 850-m station, the top 2–4 cm of sediment were riddled with burrows yielding a very low-density layer; numerous cirratulid mudballs protruded above the mean sediment–water interface. Below 4 cm, sediment density increased but remained heavily bioturbated. Sediments at the 1000-m station appeared to be denser than at shallower stations and relatively homogenous throughout the top 10 cm, with numerous hair-like burrows, and an occasional large maldanid-polychaete burrow complex (Fig. 5). One X-radiograph exhibited faint lamination in the top centimeter of sediment. At 1250 m, sediments were quite homogenous, with numerous burrows of a variety of types and sizes penetrating 4–13 cm below the sediment–water interface. At 3400 m, sediments were relatively low in density and riddled with open burrows to 4–7 cm depths; two cores exhibited laminations at 12–14 cm suggestive of a turbidite.

Table 5
Mean ^{210}Pb mixed-layer depth and D_b from the Arabian Sea OMZ (400–1000 m depths) and from oxygenated slopes on other continental margins at similar depths (375–1275 m depths). The mean mixed-layer depths from the Arabian Sea OMZ and the combined oxygenated slopes differ significantly ($p < 0.05$, t test); the mean D_b's for the OMZ and oxygenated slopes were not significantly different

Location	Water depth (m)	Bottom-water oxygen (ml l^{-1})	Mean mixed-layer depth ± s.e. (cm)	Mean D_b ± s.e. (cm^2 y^{-1})	Reference
Arabian slope OMZ	400–1000	0.13–0.27	4.6 ± 0.2	1.1 ± 0.62	This study
Eastern Australian slope	376–990	> 4	—	0.93 ± 0.65	Heggie et al. (1990)
North Carolina slope	850	> 4	11 ± 3.5	1.39 ± 0.71	Pope et al. (1996)
Northwest Atlantic slope	500–1275	> 4	10 ± 1.2	0.6 ± 0.1	Anderson et al. (1988)
Santa Catalina Basin	1250	~ 0.5	12 ± 0.6	0.74 ± 0.22	Pope et al. (1996)
Oxygenated-slope mean			11.1 ± 0.5	0.90 ± 0.32	

Table 6
Characteristics of open burrows and sediment fabric visible in X-radiographs. One to two X-radiographs were obtained from each sample

Station and sample no.	Maximum burrow diameter (cm)	Modal burrow diameter (cm)	Number of burrow types	Penetration depth of burrows (cm)	Comments
400 m					
12690/3	0.1	~ 0.05	1	4	Numerous very fine vertical burrows in top 2 cm; faint cm-scale laminae visible from ~ 2–3 cm, otherwise well mixed to 12 cm
12692/4	0.1	~ 0.05	2 (only 1 common)	8–10 cm (modal fine burrows to 8–9 cm)	Numerous very fine burrows at 4–8 cm depths; a few fine vertical burrows in top 2 cm; top 3 cm with cm-scale laminations, otherwise well mixed; only one example of larger burrow
12695/7	0.3	~ 0.05	2 (only 1 common)	10 cm? (fine burrows to ~ 4 cm)	Burrows rare with a few very faint fine burrows (0.05 cm diameter) in top 3–5 cm; two larger (0.3 cm) burrows at 5 and 10 cm; very faint cm-scale laminations in top 2 cm. (Total number of burrow types at 400 m = 2)
700 m					
12685/6	0.5	~ 0.1	3 (only 1 common)	8–10 cm (modal fine burrows to 3–4 cm)	Top 3 cm lower in density with numerous mm-scale vertical burrows, many ending in protruding tubes; several quasi-horizontal 5-mm diameter, walled tubes in top 2 cm; some mottling at 5–10 cm; dramatic switch in density of sediment at 4–8 cm (horizon irregular)
12685/8	0.3	0.05–0.1	3 (only 1 common)	5.2	Lower density sediment in top 6–7 cm with numerous fine vertical burrows, many ending in protruding tubes; occasional horizontal tubes with well-defined walls up to 0.3 cm in diameter; faint mottling at 6–9 cm depths
12685/10	0.3	0.05–0.1	2 (only 1 common)	5.5	Numerous fine vertical burrows in top 5 cm, many ending in protruding tubes, some U shaped; occasional filled, walled tubes up to 0.5 cm diameter in top 4 cm; very faint 0.5-cm laminae visible in top 1.5 cm; dramatic shift in sediment density at 5–6 cm (horizon irregular, i.e., lumpy). (Total number of burrow types at 700 m = 3)
850 m					
12711/2	0.2	~ 0.1	2	4.5 (vast majority to 1–2 cm)	Top 1–2 cm in many areas heavily burrowed and low in density; cirratulid mudballs (7–8 per core) protrude 0.5–1 cm above, and 1–1.5 cm below interface; amphipods ~ 0.7 cm in length visible to 5-cm depths; between ~ 2 and 10-cm depths, sediment is quite homogeneous

12713/1	0.2	0.1–0.15	3	4.5 (most burrows in top 3 cm)	Numerous mm-scale burrows in top 3 cm yielding highly bioturbated sediment; occasional open vertical burrows (0.2 mm diameter) to 2 cm, and occasional cm-scale cirratulid mudballs protruding 0.5–1.0 cm above and below the interface; burrows diminish and sediment gradually increases to 4–5 cm depth; below 5 cm, sediment quite homogeneous with an occasional 0.2–0.3 mm diameter tube
12713/4	0.5	~ 0.1	3	10 (vast majority to < 4)	Top 2–4 cm riddled with mm-scale burrows; numerous cirratulid mudballs protruding 0.5 cm above and 1.0 cm below interface; below 4–5 cm sediment denser and relatively homogeneous with occasional mm-scale burrow
12715/1	0.2	~ 0.1	3	12 (most burrows < 4 cm)	Moderate number of mm-scale burrows in top 2–3 cm, these become much less common deeper, but a few visible at 10–12 cm; occasional cm-scale pits and cirratulid mudballs near interface; below 2–3 cm sediment quite homogeneous. (Total number of burrow types at 850 m = 3)
1000 m					
12716/2	0.15	< 0.1	2	5 cm	Sediment relatively dense and homogenized throughout; convolute maldanid tube complex penetrating to 3.5 cm; low density of very fine, hairlike burrows from depths of 1–5 cm; cm-scale mottling possibly from relict burrows below 7 cm
12718/2	< 0.1	< 0.1	1	6.5 cm (vast majority < 4 cm)	Sediment relatively dense and homogeneous throughout; moderate density of hairlike burrows at depths of 1–4 cm; occasional cm-scale relict horizontal burrows below 9 cm
12718/4	< 0.1 (filled maldanid tubes 0.2)	< 0.1	1	7 (most < 5)	Sediment relatively dense and homogeneous throughout; top cm denser than immediately underlying layers and poorly burrowed; moderate number of hairlike burrows from 1–5 cm; occasional filled, convolute maldanid-tube complexes penetrating to 3.5 cm
12722/1	~ 0.1	< 0.1	2	7 cm (most < 5)	Sediment relatively dense and homogeneous throughout; occasional 0.1-cm diameter vertical burrows penetrating to 1.5 cm; moderate number of hairlike burrows to 5 cm; mottling from filled cm-scale horizontal burrows from 2–10 cm. Some faint lamination in the top cm. (Total number of burrow types at 1000 m = 3)
1250 m					
12723/2	0.5	< 0.1	4	13 (most < 4)	Relatively dense, homogeneous sediment; moderate number of hairlike burrows in top 4 cm; occasional conical burrows extending from surface to 1–3 cm; occasional helical burrows 0.1 cm in diameter in top 3 cm; a few 0.3 cm burrow segments at ~ 13 cm depth

Table 6 (*continued*)

Station and sample no.	Maximum burrow diameter (cm)	Modal burrow diameter (cm)	Number of burrow types	Penetration depth of burrows (cm)	Comments
12723/4	0.2	0.1	4	7.5 (most < 5)	Relatively homogeneous sediment with lower density patches in top cm; moderate number of vertical burrows 0.1–0.2 cm in diameter extending from surface to depths of 5–7 cm; occasional helical burrow ~0.15 cm in diameter at 5–7 cm depth; anastomosing mm-scale burrows common at depths of 1–4 cm
12725/2	0.5	0.1–0.2	4	10 (most < 5)	Relatively homogeneous sediment; occasional vertical, 0.5 cm burrows penetrating to 10 cm; moderate number of vertical burrows 0.2 cm in diameter in top 2 cm and branching, mm-scale horizontal burrows from 1–3 cm
12725/4	0.5	0.1–0.2	5	9 (most < 6)	Low density layer (0.3–0.5 cm thick) atop relatively dense, homogeneous sediment; moderate number of mm-scale vertical tubes extending from surface to ⩾6 cm; burrow types include (a) conical cm-scale surface burrow, (b) 0.3 by 4 cm protruding tube, (c) hairlike burrow networks, (d) 0.2 cm diameter helical burrows, (e) mm-scale vertical tubes. (Total of seven different burrow types at 1250 m)
3400 m					
12671/4	0.3	0.2	2	10 (most < 7 cm)	Relatively low density, homogeneous sediment with numerous horizontal burrows ~0.2 mm in diameter in top 7 cm; occasional hairlike vertical burrows in top cm; arenaceous tests common at depths of 0–4 cm
12688/1	0.5	0.2	4	9 (most < 6)	Relatively low-density, heavily burrowed, homogeneous sediment to 12–13 cm; high-density, laminated turbidite occurs at ~12–14 cm; occasional 0.2 cm diameter vertical burrow from 0–2 cm; abundant horizontal and slanting burrows of 0.1–0.2 cm diameter from 0.5 to 6 cm depths; occasional 0.5 cm diameter, horizontal burrow from 0 to 9 cm depths; arenaceous/calcareous tests and shells occur in top 4 cm
12687/4	1.0	0.1	4	11 (most < 6)	Relatively low-density, heavily burrowed, homogeneous sediment to 12–13 cm; high-density, laminated turbidite occurs at ~12–14 cm; numerous 0.1–0.2-cm diameter vertical burrows from 0 to 2 cm; abundant horizontal and slanting burrows of 0.1–0.2 cm diameter from 0.5 to 6 cm depths; 1.0 cm diameter burrow at 11 cm. (Total types of burrows at 3400 m = 5)

Maximum burrow diameter, modal burrow diameter, and burrow diversity all varied along the Oman-slope transect (Table 4). However, the only significant difference in maximum burrow diameter occurred between the 1000 and 1250-m stations, with diameter greater at 1250 m (Table 4). Maximum burrow diameter was not significantly correlated with bottom-water oxygen concentration (Spearman rho = 0.3, $p > 0.30$). Modal burrow diameter and the number of burrow types per core (or local burrow diversity) exhibited more orderly patterns, generally increasing from the center to the edge of the OMZ (i.e., from 400 to 1250 m, Fig. 6). In addition, both modal burrow diameter and total number of burrow types per station (Table 7; Fig. 7) exhibited significant positive correlation with bottom-water oxygen concentrations from 400 to 1250 m (Spearman rho's of 0.90 and 0.89, respectively, with p levels $\leqslant 0.02$). Neither maximum nor modal penetration depths of burrows exhibited significant pattern with depth or oxygen concentration along our transect.

3.3. Macrofaunal patterns

As described in detail in Levin et al. (2000), macrofaunal densities and biomass varied among stations. Total macrofaunal densities were highest at 700 and 850 m (19,000 and 17,000 m^{-2}), respectively, intermediate at the 400-m station (12,000 m^{-2}), and lowest at 1000, 1250 and 3400 m (3000–8000 m^{-2}). Biomass was highest at 700 m (59 g m^{-2}) and differed significantly from the 400, 1250 and 3400 m stations (4.2–14 g m^{-2}).

The vertical distributions of macrofaunal abundance (Fig. 8) and biomass (Fig. 9) within the sediment column also varied among stations. The 400 and 700 m stations had a significantly greater number of individuals collected below 5 cm, while the 700 m station had significantly higher biomass below 5 cm than all other stations (Table 4). Contrary to the expectation that deeper faunal penetration would promote deeper mixing, these were the stations with the shallowest ^{210}Pb mixed-layer depths.

The proportional representation of macrofauna in different depth fractions (normalized to the total within each core) revealed somewhat different patterns. The proportion of individuals below 5 cm at the 3400, 400 and 1250 m stations (0.12–0.29) was dramatically higher than at 1000 m (0.01). The proportion of individuals dwelling below 10 cm was higher at 3400 m (0.12) than at all other stations (0–0.02). The proportional distribution of biomass exhibited little pattern; only biomass below 5 cm at 850 m (0.40) substantially exceeded that at 1000 m (0.07).

Life styles of macrofauna shifted substantially across the transect. Within the OMZ (400–1000 m stations), tube dwellers, including spionid, ampharetid, sabellid and some cirratulid polychaetes, as well as cocoon-forming mussels, constituted $> 50\%$ of the macrofauna. In contrast, at the OMZ boundary and in the abyss (the 1250 and 3400-m stations), tube dwellers constituted $< 32\%$ of the fauna.

Feeding modes of polychaetes (the predominant macrofaunal taxon) also shifted substantially along the Oman margin transect. Surface-deposit feeding polychaetes dominated macrofaunal assemblages within the OMZ, constituting $> 85\%$ of

abundance. At the 400–700 m stations spionids and cirratulids were the predominant surface deposit feeders, while paranoids and ampharetids dominated at 850–1000 m. At the OMZ boundary and abyssal stations, subsurface-deposit feeders plus

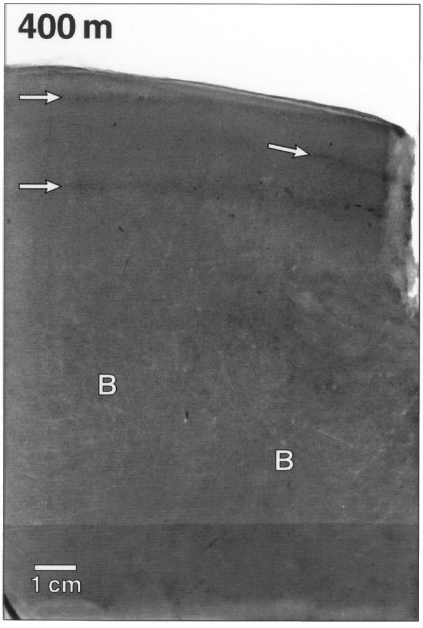

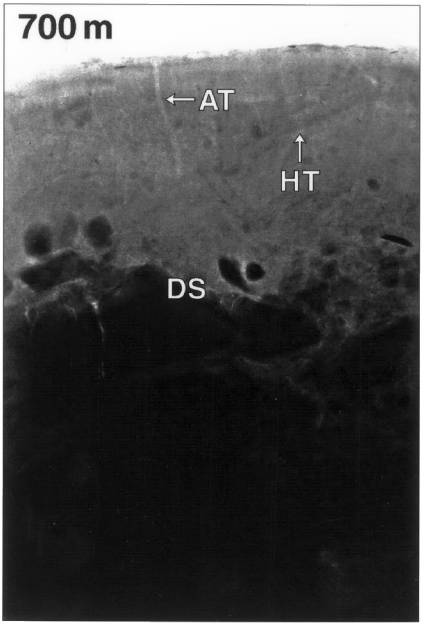

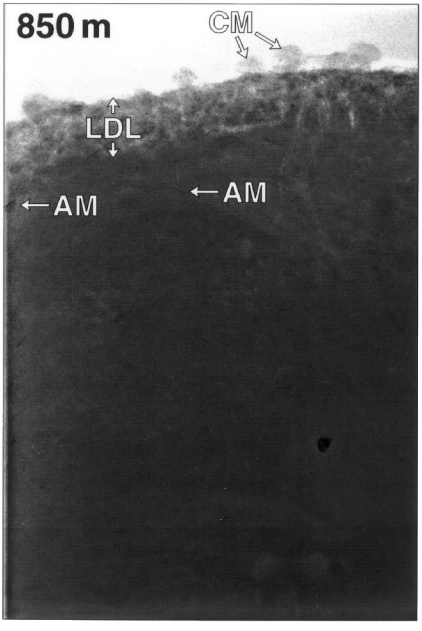

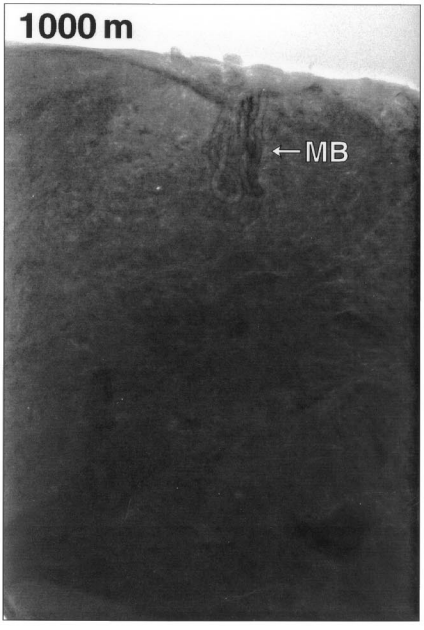

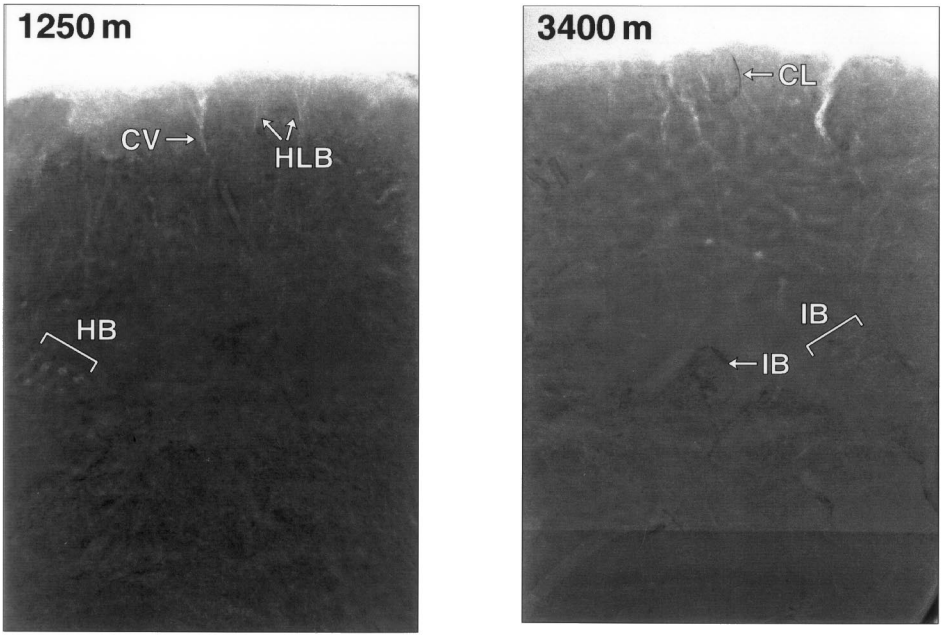

Fig. 5 (*continued*)

carnivores where roughly equivalent in importance to surface-deposit feeding polychaetes, constituting on average $>45\%$ of the macrofauna. For more details concerning life styles and feeding modes, see Levin et al. (2000).

Fig. 5. Representative X-radiographs from box cores collected at our Oman-margin stations at 400, 700, 850, 1000, 1250 and 3400 m. The scale is identical for all X-radiographs (note scale bar on 400-m plate). For detailed description of X-rays, see Table 6. **400 m (sample no. 12692/4):** Centimeter-scale laminations in the top 2 cm with (arrows) a few very faint fine burrows (0.05 cm diameter) from 4 to 8 cm (e.g., in areas indicated by B's). **700 m (sample no. 12685/10):** Numerous fine burrows in the top 5–6 cm, with many (ampeliscid amphipod tubes, AT) ending in protuding tubes. Note the 0.5-cm diameter nearly horizontal tube in the upper right (HT), and the dramatic shift in sediment density along an irregular horizon at 6–7 cm depths (DS). **850 m (sample no. 12711/2):** Very abundant millimeter-scale burrows in top 2–3 cm produce a low-density layer (LDL). Note the cirratulid mudballs (CM) protruding ~ 1 cm above and below the sediment–water interface (see Levin and Edesa, 1997 for a description), and the homogeneous nature of the sediment. The dark, horizontal, centimeter-scale "parentheses" marks in the top 3–4 cm are the dorsal surfaces of ampipods (AM). **1000 m (sample no. 12716/2):** Relatively homogeneous sediment with very fine, hairlike burrows in top 1–5 cm, and a convolute maldanid burrow complex (MB) penetrating from the sediment surface to 3.5 cm. **1250 m (sample no. 12723/4):** Note the numerous hairlike burrows (HLB), and the occasional conical vertical burrows (CV; probably from ampharetids) in the top 4 cm. Also note the centimeter-scale helical burrow (HB) probably formed by a paranoid, and the relatively homogeneous nature of the sediment. **3400 m (sample no. 12687/4):** Numerous horizontal and vertical burrows ranging from 0.1 to 0.5 cm in diameter throughout top six centimeters. Note the 1.5 cm long clam (CL) at the sediment surface, and larger infilled centimeter-scale burrows at 8–11 cm (IB).

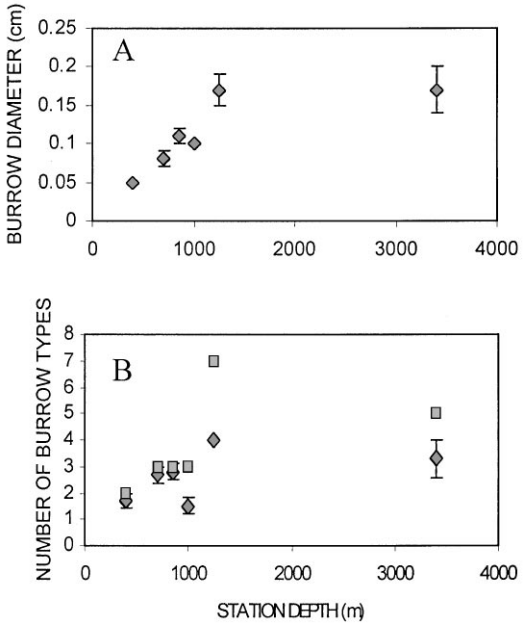

Fig. 6. (A) Modal burrow diameter, and (B) mean number of burrow types per sample (diamonds) and total number of burrow types at a station (squares) versus depth on the Oman slope. Error bars are ± one standard error.

3.4. Exploratory regressions

Least-squares regression analysis was used to explore relationships between bioturbation and the macrofaunal parameters described above. Specifically, relationships were explored between (a) ^{210}Pb D_b, ^{210}Pb mixed-layer depth, maximum burrow depth, maximum burrow diameter, and total number of burrow types per station, and (b) macrofaunal abundance, biomass, average body size, abundance below 5 cm, and average body size below 5 cm. In addition, relationships between total burrow types per station and various macrofaunal indices of diversity (i.e., rarefaction diversity at 100 individuals or ES(100), and H' and J' on $\log_2$; Levin et al., 2000) were investigated. Those regressions yielding p levels near or below 0.05 are listed in Table 8.

These analyses revealed little or no relationship between macrofaunal parameters and ^{210}Pb mixing intensity and mixed-layer depth; only the regression of D_b versus biomass had a nearly significant p level (Table 8), with the direction of the relationship unexpectedly negative. Also to our surprise, maximum burrow depth evident in X-radiographs was negatively related to macrofaunal abundance and biomass. More expectedly, the total number of burrow types within a station was strongly positively related to all three macrofaunal diversity parameters (ES(100), H', and J'); total number of burrow types also was negatively correlated with macrofaunal density.

Table 7
Quantitative results from analyses of X-radiographs on the Arabian Slope

Water depth in meters (no. of replicates)	$\bar{x}_{max}$ burrow diameter (cm)	$\bar{x}$ modal burrow diameter (cm)	$\bar{x}$ number of burrow types per core	Total burrow types in depth zone	$\bar{x}_{max}$ burrow penetration depth (cm)	$\bar{x}$ modal burrow penetration depth (cm)
400 ($n = 3$)	0.17 ± 0.07	0.05 ± 0	1.7 ± 0.3	2	8.0 ± 2.0	5.6 ± 1.7
700 ($n = 3$)	0.36 ± 0.07	0.08 ± 0.01	2.7 ± 0.3	3	6.9 ± 1.5	4.9 ± 0.5
850 ($n = 4$)	0.28 ± 0.08	0.11 ± 0.01	2.8 ± 0.3	3	7.8 ± 1.9	3.3 ± 0.4
1000 ($n = 4$)	0.11 ± 0.01	0.1 ± 0	1.5 ± 0.3	3	6.4 ± 0.5	4.8 ± 0.3
1250 ($n = 3$)	0.4 ± 0.1	0.17 ± 0.02	4 ± 0	7	10.2 ± 1.6	4.7 ± 0.3
3400 ($n = 3$)	0.60 ± 0.21	0.17 ± 0.03	3.3 ± 0.7	5	10.0 ± 0.6	6.3 ± 0.3
OMZ: 400–1000 ($n = 4$)	0.23 ± 0.06[a]	0.09 ± 0.01	2.1 ± 0.3	2.8 ± 0.3	7.2 ± 0.4	4.7 ± 0.5
Non OMZ: 1250–3400 ($n = 2$)	0.5 ± 0.10[a]	0.17 ± 0	3.7 ± 0.4	6.0 ± 1.0	10.1 ± 1.0	5.5 ± 0.8

[a]These means differ significantly ($p < 0.02$, t test); the remaining sets of means for the OMZ and non-OMZ data do not differ significantly at $\alpha = 0.05$.

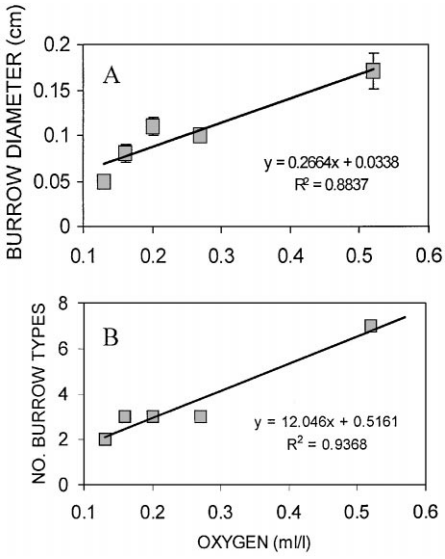

Fig. 7. (A) Modal burrow diameter and (B) total number of burrow types at each station versus bottom-water oxygen concentration. Equations and r^2 values for the regression lines are given. Error bars are $\pm$ one standard error.

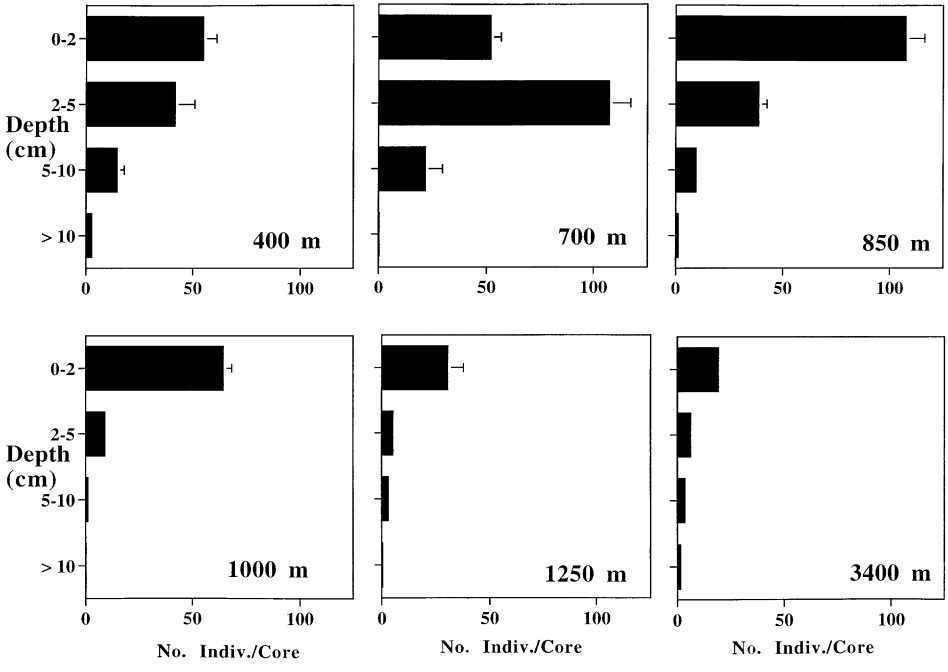

Fig. 8. Mean vertical distributions of macrofaunal abundance in box-core samples from Oman-slope stations. Error bars are $\pm$ one standard error.

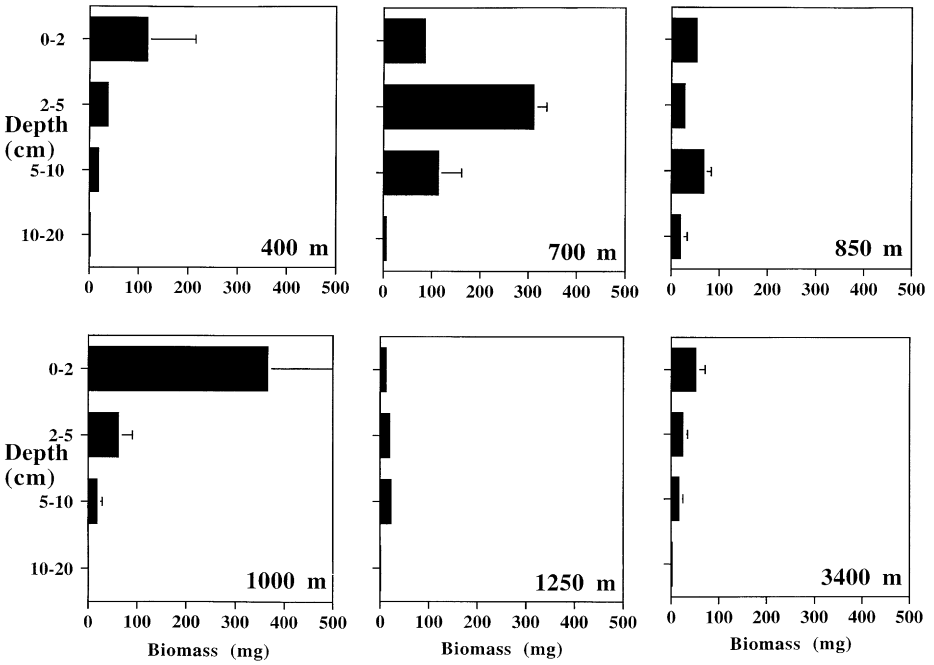

Fig. 9. Mean vertical distributions of macrofaunal biomass in box-core samples from Oman-slope station. Error bars are ± one standard error.

Table 8
Results from exploratory regression analyses on $\log_{10}$-transformed data. Explanations for the calculation of diversity (rarefaction at 100 individuals or ES(100), H', and J' are given in Levin et al. (2000))

Dependent variable	Independent variable	r^2	p level	Direction
Linear regressions				
D_b	Macrofaunal biomass	0.63	0.06	Negative
Maximum burrow depth	Macrofaunal biomass	0.592	0.073	Negative
	Macrofaunal abundance	0.867	0.007	Negative
Total no. of burrow types per station	Macrofaunal abundance	0.687	0.041	Negative
	ES(100)	0.807	0.015	Positive
	H′	0.754	0.025	Positive
	J′	0.749	0.026	Positive
Second-order polynomial regressions				
Maximum burrow diameter	Macrofaunal density	0.899	0.032	Concave
	Average macrofaunal body size	0.875	0.044	Convex
	Average macrofaunal body size below 5 cm	0.943	0.014	Convex

4. Discussion

We postulated (hypothesis no. 1) that ^{210}Pb mixed-layer depth and D_b would be maximal at the OMZ boundary (i.e., roughly at the 1250 m station), where bottom-water oxygen concentration just exceeded the lower limits of burrowing and bioturbating fauna, and faunal densities were enhanced by organic matter sinking from the OMZ. Although macrofaunal abundance maxima occurred at 700–850 m (i.e., at bottom water oxygen values of ~ 0.16–$0.20\ ml\ l^{-1}$), most of the animals at these stations were surface feeders (Levin et al., 2000) and apparently did not produce particularly intense vertical mixing. Subsurface-deposit feeders did become prominent at 1250 m (oxygen $\sim 0.5\ ml\ l^{-1}$), but there was no clear enhancement of bioturbation at this station either, possibly because macrofaunal standing crop was relatively low. These bioturbation results contrast those of Mullins et al. (1985) from the northeast Pacific slope, where there was evidence of enhanced bioturbation at the OMZ boundary. Bioturbation activities near the lower OMZ boundary on the Oman slope could be low compared to the other studied OMZ's because the oxygen gradient at the bottom of the Oman OMZ is relatively gradual, or because physical transport processes (e.g., mass wastage or hydrodynamic winnowing) prevent seafloor accumulation of organic matter sinking from the OMZ. Sediments were in fact coarser and lower in organic matter near the OMZ boundary (1000–1250 m) than at shallower depths on the Oman slope (Table 2; Smallwood et al., 1999), suggesting that winnowing could prevent accumulation of labile organic matter exported from the core of the OMZ (Meadows et al., 2000). Whatever the cause, our data indicate that the lower boundaries of OMZ's are not invariably regions of enhanced bioturbation.

While ^{210}Pb mixed-layer depth did not decrease into the OMZ on the Oman slope, the lack of change along the transect could result from the confounding effects of water-column depth on bioturbation. Our relatively oxygenated stations (1250 and 3400 m) were also our deepest, and the decreases in carbon flux, infaunal biomass and body size associated with changes in water depth are very likely to reduce the thickness of the sediment mixed layer (Smith, 1992; Rabouille and Smith, submitted). The mean ^{210}Pb mixed-layer depth (4.6 ± 0.2 cm) for the pooled Arabian-Sea OMZ stations (400–1000 m) was half that for oxygenated slopes at similar depths in the Atlantic and Pacific (Table 5), suggesting that bottom-water oxygen concentrations between ~ 0.10 and $\sim 0.3\ ml\ l^{-1}$ reduced the depth of ^{210}Pb mixing on the Oman slope. Kim and Burnett (1988) found similarly thin ^{210}Pb mixed layers at bathyal depths within the OMZ on the Peru margin, although their lack of oxygen data makes a direct comparison to our study difficult. In addition, the mixed-layer depth within the Oman OMZ was only half the global mean for bioturbated sediments (9.8 cm) reported by Boudreau (1994). Thus, we conclude that the mixed layer is substantially reduced in the Arabian Sea OMZ. This reduction in mixed-layer depth seems likely to result directly from the stress of low bottom-water oxygen on bioturbating benthos (see review by Diaz and Rosenberg, 1995), although secondary effects of the OMZ on bioturbation cannot be ruled out. For example, OMZs appear to reduce water-column consumption or degradation of sinking organic matter (Karl and Knauer, 1994; Wishner et al., 1990,1995). The resulting enhanced flux of labile particulate

organic carbon to OMZ sediments is likely to increase sediment oxygen demand, causing a shoaling of oxygen penetration and bioturbation activity in OMZs compared to oxygenated slopes.

In contrast, the mean D_b'*s* within the surface mixed layer did not differ between the Arabian OMZ and the oxygenated Atlantic and Pacific slopes (Table 5). Thus, the intensity of mixing per unit volume of mixed layer was similar in low-oxygen and oxygenated bathyal settings, but the mixing was restricted to only half the sediment thickness within the OMZ (Table 5). Thus, twice as much bioturbation energy appeared to be expended over the entire sediment column within the oxygenated-slope communities as in the Oman-slope OMZ. Because bioturbation activity can stimulate microbial metabolism and enhance the mineralization of organic matter through redox oscillation (e.g., Aller, 1994), reduced bioturbation could promote greater burial efficiency of organic carbon in OMZ sediments. However, whether organic carbon is more efficiently buried in OMZ sediments remains controversial (Calvert and Pederson, 1992; Pederson et al., 1992; Aller, 1994).

Our second hypothesis, derived largely from oxygen-biofacies models (e.g., Savrda and Bottjer, 1991), was that burrow diameter, diversity and penetration depth would be positively correlated with bottom-water oxygen concentration from the boundary to the core of the Oman-margin OMZ (i.e., within the 400–1250 m stations where bottom-water oxygen was $\leqslant 0.5\,\mathrm{ml\,l^{-1}}$). Both modal burrow diameter (i.e., the diameter of the most common burrow type) and the diversity of burrow types per station were strongly correlated with bottom-water oxygen levels, suggesting that they are good indicators of oxygen concentration. It should be noted that these correlations were largely driven by differences between the boundary station (1250 m) and stations closer to the core of the OMZ (i.e., 400–1000 m; Fig. 6). In contrast, burrow penetration and maximum burrow diameter showed no such relationship. Based on the sharp reduction in burrow diversity between our 1250 and 1000 m stations, and the occurrence of faint laminations (i.e., incomplete bioturbation) at our 400-m station, our 400 to 1000-m OMZ stations span the dysaerobic zone of Savrda and Bottjer (1991), and the bottom-water oxygen concentrations within this zone (~ 0.1– $\sim 0.3\,\mathrm{ml\,l^{-1}}$) are similar to those reported by Savrda and Bottjer for modern dysaerobic assemblages. Thus, our results provide support for certain components of the current oxygen-related biofacies model (Savrda and Bottjer, 1991), in particular that modal burrow size and diversity decline under oxygen concentrations thought to produce "dysaerobic" conditions. Our data also suggest that burrow diversity might be used to predict macrofaunal species diversity in dysaerobic assemblages. In contrast to current biofacies models, burrow penetration depth and maximum burrow diameter do not appear useful for predicting seafloor oxygen concentrations in dysaerobic settings.

Our findings, combined with those of Levin et al. (2000), also shed light on shifts in trace fossil types as bottom-water oxygen declines. From the boundary to the core of the Oman-margin OMZ, we see a trend of decreasing modal burrow diameter and diversity, as well as a shift from subsurface deposit feeders to surface feeding functional groups. Both trends suggest that trace fossils formed by these assemblages would exhibit decreasing occurrence of fodinichnia (subsurface- feeding traces), and

increasing dominance of pascichnia (surficial-sediment-grazing traces) as bottom-water oxygen concentrations decline. Thus, our results support the trace-fossil model of Wheatcroft (1989) and closely parallel results from organically enriched shallow-water assemblages, in which small, surface-deposit-feeding tube-dwellers frequently dominate organic-rich (and oxygen poor) sediments (e.g., Pearson and Rosenberg, 1978; Rhoads et al., 1978; Weston, 1990).

In our third hypothesis, we postulated that changes in bioturbation within the OMZ would be correlated with a shoaling in the depth distribution of macrofauna, decreases in macrofaunal abundance and biomass, and a shift to surface-oriented life-styles near the core of the OMZ. Only the latter part of this hypothesis is supported because the factors causing any shoaling of the ^{210}Pb mixed-layer in the Arabian-Sea OMZ appear to be related to faunal lifestyles, rather than to patterns (e.g., decreases) of faunal abundance and biomass. Macrofaunal abundance and biomass (both total and that below 5 cm) at Oman-slope OMZ stations were high compared to deeper, well-oxygenated sites along the transect, and compared to oxygenated slopes in other regions (see Levin et al., 2000, for more discussion); higher macrofaunal standing stock, especially below 5 cm, might be expected to enhance, rather than reduce, OMZ mixed-layer depths. However, the Oman-margin OMZ stations, in consonance with other low-oxygen slopes, exhibit an unusual predominance of tube-dwellers and surface-deposit feeders when compared to oxygenated slopes (Levin et al., 2000). The concentration of deposit-feeding activity near the sediment–water interface, combined with reduced mobility in tube dwellers, can very reasonably explain a shallow mixed layer within the Oman-slope OMZ. In a study of an organic enrichment gradient on the California shelf, Wheatcroft and Martin (1996) found similarly very weak or inverse relationships between bioturbation and macrofaunal standing stock and depth distributions. These results highlight the need for natural-history information and mechanistic studies, as opposed to simple tabulations of abundance and biomass, for predicting the effects of organisms on bioturbation and other sediment geochemical processes. Thus, as in many terrestrial soil ecosystems (e.g., Groffman and Bohlen, 1999), knowledge of the functional diversity of infauna appears to be essential to predicting the nature of bioturbation and its impacts on microbial metabolism and sediment geochemistry.

Acknowledgements

We thank many people for contributing to the field aspects of this program, including A. Patience, A. Gooday, B. Bett, and G. Wolff, as well as the entire scientific party and crew of *Discovery* Cruise 211. C. Martin and P. Lamont assisted substantially at sea and in the laboratory. M. Cremer painstakingly conducted the ^{210}Pb and porosity analyses. Support for this research was provided to CRS and LAL by the US NSF International Program (INT 94-14397), and by US NSF grant OCE 95-21116 to CRS. This is contribution no. 4869 from the School of Ocean and Earth Science and Technology, University of Hawaii at Manoa.

References

Aller, R.C., 1982. The effects of macrobenthos on chemical properties of marine sediment and overlying water. In: McCall, P.L., Tevesz, M.J.S. (Eds.), Animal Sediment Relations. Plenum, New York, pp. 53–102.

Aller, R.C., 1990. Bioturbation and manganese cycling in hemipelagic sediments. In: Charnock, H., et al. (Ed.), The Deep Sea Bed: Its Physics, Chemistry, and Biology. Cambridge University Press, Cambridge, pp. 51–68.

Aller, R.C., 1994. Bioturbation and remineralization of sedimentary organic matter: effects of redox oscillation. Chemical Geology 114, 331–345.

Anderson, R.F., Bopp, R.F., Buesseler, K., Biscaye, P., 1988. Mixing of particles and organic constituents in sediment from the continental shelf and slope off Cape Cod: SEEP – I results. Continental Shelf Research 8, 925–946.

Barnett, P.R.O., Watson, J., Connelly, D., 1984. The multiple corer for taking virtually undisturbed samples from shelf, bathyal and abyssal sediments. Oceanologica Acta 7, 277–287.

Boudreau, B.P., 1994. Is burial velocity a master parameter for bioturbation? Geochimica et Cosmochimica Acta 58, 1243–1249.

Burkill, P., 1998. Arabesque Data Set. In: CD Rom electronic publication, British Oceanographic Data Centre. Birkenhead, United Kingdom.

Calvert, S.E., Pederson, T.F., 1992. Organic carbon accumulation and preservation in marine sediments: how important is anoxia?. In: Whelan, J.K., Farrington, J. (Eds.), Organic Matter: Productivity, Accumulation and Preservation in Recent and Ancient Sediments. Columbia University Press, New York, pp. 231–263.

Diaz, R.J., Rosenberg, R., 1995. Marine benthic hypoxia, A review of its ecological effects and the behavioural responses of benthic macrofauna. Oceanography and Marine Biology, an Annual Review 33, 245–303.

Dixon, W.J., Massey Jr., F.J., 1969. Introduction to Statistical Analysis. McGraw-Hill, New York, 638pp.

Ekdale, A.A., Mason, T.R., 1988. Characteristic trace-fossil associations in oxygen-poor sedimentary environments. Geology 16, 720–723.

Ekdale, A.A., Mason, T.R., 1989. Commentary and reply on "Characteristic trace-fossil associations in oxygen-poor sedimentary environments". Geology 17, 674–676.

Emerson, S., 1985. Organic carbon preservation in marine sediments. In: Sundquist, L., Broecker, W. (Eds.), The Carbon Cycle and Atmospheric CO_2: Natural Variations Archean to Present, Vol. 32. Geophysical Monograph, AGU, Washington, DC, pp. 78–87.

Graf, G., 1989. Benthic-pelagic coupling in a deep-sea benthic community. Nature 341, 437–439.

Groffman, P.M., Bohlen, P.J., 1999. Soil and sediment biodiversity. Bio Science 49, 139–148.

Hammond, D.E., McManus, J., Berelson, W.M., Kilgore, T.E., Pope, R.H., 1996. Early diagenesis of organic material in Equatorial Pacific sediments: stoichiometry and kinetics. Deep-Sea Research II 43, 1365–1412.

Heggie, D.T., Skyring, G., O'Brien, G., Reimers, C., Herczeg, A., Moriarity, D., Burnett, W., Milnes, A., 1990. Organic carbon cycling and modern phosporite formation on the East Australian continental margin: an overview. In: Notholt, A., Jarvis, I. (Eds.), Phosphorite Reseach and Development, Vol. 52. Geol. Society Special. Pub, pp. 87–117.

Jumars, P.A., Nowell, A.R.M., 1984. Flow environments of aquatic benthos. Annual Review of Ecology and Systematics 15, 303–328.

Karl, D.M., Knauer, G.A., 1984. Vertical distribution, transport and exchange of carbon in the northeast Pacific Ocean. Evidence for multiple zones of biological activity. Deep-Sea Research 31, 221–243.

Kim, K.H., Burnett, W.C., 1983. Gamma-ray spectrometric determination of uranium series nuclides in marine phosphorites. Analytical Chemistry 55, 1796–1800.

Kim, K.H., Burnett, W.C., 1988. Accumulation and biological mixing of Peru margin sediments. Marine Geology 80, 181–194.

Kim, K.H., McMurtry, G.M., 1991. Radial growth rates and ^{210}Pb ages of hydrothermal massive sulfides from the Juan de Fuca Ridge. Earth and Planetary Science Letters 104, 299–314.

Kramer, K., Misdorp, R., Berger, G., Duijts, R., 1991. Maximum pollution concentrations at the wrong depth: a misleading pollution history in a sediment core. Marine Chemistry 36, 183–198.

Levin, L., Blair, N., DeMaster, D., Plaia, G., Fornes, W., Martin, C., Thomas, C., 1997. Rapid subduction of organic matter by maldanid polychaetes on the North Carolina Slope. Journal of Marine Research 55, 595–611.

Levin, L., Edesa, S., 1997. The ecology of cirratulid mudballs on the Oman Margin. Marine Biology 128, 671–678.

Levin, L.A., Gage, J.D., Martin, C., Lamont, P.A., 2000. Macrobenthic community structure within and beneath the oxygen minimum zone, NW Arabian Sea. Deep-Sea Research II 47, 189–226.

Levin, L.A., Huggett, C.L., Wishner, K.F., 1991. Control of deep-sea benthic community structure by oxygen and organic-matter gradients in the eastern Pacific Ocean. Journal of Marine Research 49, 763–800.

Lipschultz, F., Wofsy, S.C., Ward, B.B., Codispoti, L., Friedrich, G., Elkins, J., 1990. Bacterial transformations of inorganic nitrogen in the oxygen-deficient waters of the Eastern Tropical South Pacific Ocean. Deep-Sea Research 37, 1413–1541.

Meadows, A., Meadows, P.S., West, F.C., Murray, J.M.H., 2000. Bioturbation, geochemistry and geotechnics of sediments affected by the oxygen minimum zone on the Oman continental slope and abyssal plain, Arabian Sea. Deep-Sea Research II 47, 259–280.

Mullins, H.T., Thompson, J.B., McDougall, K., Vercoutere, T.L., 1985. Oxygen-minimum zone edge effects, evidence from the central California coastal upwelling system. Geology 13, 491–494.

Nittrouer, C.A., DeMaster, D.J., McKee, B.A., Cutshall, N.H., Larsen, I.L., 1983/84. The effect of sediment mixing on ^{210}Pb accumulation rates for the Washington continental shelf. Marine Geology 54, 210–221.

Pearson, T.H., Rosenberg, R., 1978. Macrobenthic succession in relation to organic enrichment and pollution in the marine environment. Oceanography and Maine Biology Annual Review 16, 229–311.

Pederson, T.F., Shimmield, G.B., Price, N.B., 1992. Lack of enhanced preservation of organic matter in sediments under the oxygen minimum on the Oman margin. Geochimica et Cosmochimica Acta 56, 545–551.

Pope, R.H., DeMaster, D.J., Smith, C.R., Seltmann, H., 1996. Rapid bioturbation in equatorial Pacific sediments: evidence from excess ^{234}Th measurements. Deep-Sea Research II 43, 1339–1364.

Rabouille, C., Gaillard, J.F., 1991. A coupled model representing the deep-sea organic carbon mineralization and oxygen consumption in surficial sediments. Journal of Geophysical Research 96, 2761–2776.

Rabouille, C., Smith, C.R., Controls of the mixing depth (L) in deep-sea sediments Limnology and Oceanography, submitted for publication.

Rhoads, D.C., McCall, P.L., Yingst, J.Y., 1978. Disturbance and production on the estuarine seafloor. American Scientist 66, 577–586.

Savrda, C.E., Bottjer, D.J., 1991. Oxygen-related biofacies in marine strata, An overview and update. In: Tyson, R., Pearson, T. (Eds.), Modern and ancient continental shelf anoxia. The Geological Society of London, London, pp. 201–219.

Schink, D.R., Guinasso, N.L., Fanning, K.A., 1975. Processes affecting the concentration of silica at the sediment-water interface of the Atlantic Ocean. Journal of Geophysical Research 80, 3013–3031.

Smallwood, B.J., Bett, B.J., Smith, C.R., Gage, J.D., Patience, A., Hoover, D., Wolff, G.A., 1999. Megafauna can control the quality of organic matter in marine sediments. Naturewissenschaften 86, 320–324.

Smith, C.R., 1992. Factors controlling bioturbation in deep-sea sediments and their relation to models of carbon diagenesis. In: Rowe, G.T., Pariente, V. (Eds.), Deep-Sea Food Chains and the Global Carbon Cycle. Kluwer, Netherlands, pp. 375–393.

Smith, C.R., DeMaster, D.J., Fornes, W.L., 2000. Mechanisms of age-dependent bioturbation on the bathyal California margin: the yound and the restless. In: Aller, J., Woodin, S., Aller, R. (Eds.), Organism–Sediment Interactions. University of South Carolina Press, Columbia, SC, in press.

Smith, C.R., Hoover, D.J., Doan, S.E., Pope, R.H., DeMaster, D.J., Dobbs, F.C., Altabet, M.A., 1996. Phytodetritus at the abyssal seafloor across 10° of latitude in the central equatorial Pacific. Deep-Sea Research II 43, 1309–1338.

Smith, C.R., Pope, R.H., DeMaster, D.J., Magaard, L., 1993. Age-dependent mixing of deep-sea sediments. Geochimica et Cosmochimica Acta 57, 1473–1488.

Thompson, J.B., Mullins, H.T., Newton, C.R., Vercoutere, T., 1985. Alternative biofacies model for dysaerobic communities. Lethaia 18, 167–179.

Weston, D.P., 1990. Quantitative examination of macrobenthic community changes along an organic enrichment gradient. Marine Ecology Progress Series 61, 233–244.

Wheatcroft, R.A., 1989. Comment and Reply on "Characteristic trace-fossil associations in oxygen-poor sedimentary environments". Geology 17, 674.

Wheatcroft, R.A., 1990. Preservation potential of sedimentary event layers. Geology 18, 843–845.

Wheatcroft, R.A., Jumars, P.A., Smith, C.R., Nowell, A.R.M., 1990. A mechanistic view of the particulate biodiffusion coefficient: step lengths, rest periods and transport directions. Journal of Marine Research 48, 177–207.

Wheatcroft, R.A., Martin, W.R., 1996. Spatial variation in short-term (^{234}Th) sediment bioturbation intensity along an organic-carbon gradient. Journal of Marine Research 54, 763–792.

Wishner, K., Levin, L., Gowing, M., Mullineaux, L., 1990. Involvement of the oxygen minimum in benthic zonation on a deep seamount. Nature 346, 57–59.

Wishner, K.F., Ashjian, C.J., Gelfman, C., Gowing, M., Kann, L., Levin, L., Mullineaux, L., Saltzman, J., 1995. Pelagic and benthic ecology of the lower interface of the Eastern Tropical Pacific oxygen minimum zone. Deep-Sea Research 42, 93–115.